CANCER COMMUNICATIONS Open Access

ORIGINAL ARTICLE

Enhancement of CAR-T cell activity against cholangiocarcinoma by simultaneous knockdown of six inhibitory membrane proteins

Yidan Qiao[1,2] 🆔 | Jie Chen[1] | Xuemei Wang[2] | Shumei Yan[2] | Jizhou Tan[2] |
Baijin Xia[2] | Yongjian Chen[1] | Keming Lin[2] | Fan Zou[2] | Bingfeng Liu[2] |
Xin He[2] 🆔 | Yiwen Zhang[2] | Xu Zhang[2] | Hui Zhang[2,3] | Xiangyuan Wu[1] |
Lijuan Lu[1]

[1]Department of Medical Oncology, the Third Affiliated Hospital of Sun Yat-sen University, Guangzhou, Guangdong, P. R. China

[2]Key Laboratory of Tropical Disease Control of Ministry Education, Guangdong Engineering Research Center for Antimicrobial Agent and Immunotechnology, Institute of Human Virology, Sun Yat-sen University, Guangzhou, Guangdong, P. R. China

[3]Guangzhou National Laboratory, Bio-Island, Guangzhou, Guangdong, P. R. China

Correspondence
Lijuan Lu and Xiangyuan Wu, Department of Medical Oncology, the Third Affiliated Hospital of Sun Yat-sen University, Guangzhou, Guangdong, P. R. China.
Email: lulj25@mail.sysu.edu.cn and wuxiangy@mail.sysu.edu.cn

Hui Zhang, Institute of Human Virology, Key Laboratory of Tropical Disease Control of Ministry Education, Guangdong Engineering Research Center for Antimicrobial Agent and Immunotechnology, Sun Yat-sen University, Guangzhou, Guangdong, P. R. China.

Abstract

Background: Existing treatments for cholangiocarcinoma have poor efficacy. However, chimeric antigen receptor-T (CAR-T) cells are emerging as a potential therapeutic strategy. Solid tumors possess multiple adverse factors in an immunosuppressive microenvironment that impair CAR-T cell infiltration and function. This study aimed to improve the function of CAR-T cells through knock down immune checkpoints and immunosuppressive molecular receptors.

Methods: We evaluated the expression of epidermal growth factor receptor (EGFR) and B7 homolog 3 protein (B7H3) antigens in cholangiocarcinoma tissues using immunohistochemistry and screened specific immune checkpoints in the cholangiocarcinoma microenvironment via flow cytometry. Subsequently, we engineered CAR-T cells targeting EGFR and B7H3 antigens.

List of abbreviations: CAR-T, chimeric antigen receptor T; EGFR, epidermal growth factor receptor; B7H3, B7 homolog 3; GP120, gp120 antigen; PD-1, programmed death-1; Tim-3, T-cell immunoglobulin and mucin domain-3; Tigit, T cell immunoglobulin and ITIM domain; TGFβR, Transforming growth factor β receptor; IL-10R, Interleukin-10 Receptor; IL-6R, Interleukin-6 Receptor; NGS, next-generation sequencing; FGFR2, fibroblast growth factor receptor 2; IDH-1, isocitrate dehydrogenase-1; PD-L1, programmed death-ligand 1; HER2, human epidermal growth factor receptor 2; MUC-1, mucin 1; GPC3, glypican-3; TME, tumor microenvironment; IL, interleukin; CCL21, C-C Motif Chemokine Ligand 21; CXCR, C-X-C motif chemokine receptor; PBMC, Peripheral blood mononuclear cell; BSA, bovine serum albumin; LDH, lactate dehydrogenase; TIL, tumor-infiltrating lymphocyte; RBC, red blood cell; IHC, Immunohistochemistry; HRP, Horseradish Peroxidase; IgG, immunoglobulin G; H&E, hematoxylin and eosin; scFV, single-chain fragment variable; Lag3, lymphocyte activation gene 3; BTLA, B and T lymphocyte attenuator; CTLA4, cytotoxic T lymphocyte-associated protein-4; ORR, overall response rate; MDS, myelodysplastic syndromes; HMA, hypomethylating agent; siRNA, small interfering RNA; ERBB, erythroblastic leukemia viral oncogene homolog.

Email: zhangh92@mail.sysu.edu.cn

We simultaneously knocked down immune checkpoints and immunosuppressive molecular receptors in CAR-T cells by constructing two clusters of small hairpin RNAs and evaluated the engineered CAR-T cells for antitumor activity both in vitro, using tumor cell lines and cholangiocarcinoma organoid models, and in vivo, using humanized mouse models.

Results: We observed high expression of EGFR and B7H3 antigens in cholangiocarcinoma tissues. EGFR-CAR-T and B7H3-CAR-T cells demonstrated specific anti-tumor activity. We found an abundance of programmed cell death protein 1 (PD-1), T cell immunoglobulin and mucin domain-containing protein 3 (Tim-3), and T cell immunoglobulin and ITIM domain (Tigit) on infiltrated CD8$^+$ T cells in the cholangiocarcinoma microenvironment. We then decreased the expression of these 3 proteins on the surface of CAR-T cells, named PTG-scFV-CAR-T cells. Furthermore, we knocked-down the expression of transforming growth factor beta receptor (TGFβR), interleukin-10 receptor (IL-10R), and interleukin-6 receptor (IL-6R) of PTG-scFV-CAR-T cells. Those cells, named PTG-T16R-scFV-CAR-T cells, potently killed tumor cells in vitro and promoted apoptosis of tumor cells in a cholangiocarcinoma organoid model. Finally, the PTG-T16R-scFv-CAR-T cells showed greater inhibitory effect on tumor growth in vivo, and were superior in prolonging the survival of mice.

Conclusions: Our results revealed that PTG-T16R-scFV-CAR-T cells with knockdown of sextuplet inhibitory molecules exhibited strong immunity against cholangiocarcinoma and long-term efficacy both in vitro and in vivo. This strategy provides an effective and personalized immune cell therapy against cholangiocarcinoma.

KEYWORDS
CAR-T, cholangiocarcinoma, immunosuppression, liver cancer, T cell receptor, tumor microenvironment

1 | BACKGROUND

As the second most common primary carcinoma of the liver after hepatocellular carcinoma, cholangiocarcinoma comprises highly heterogeneous biliary epithelial malignancies [1]. Surgical treatment remains the preferred treatment for patients with limited-stage cholangiocarcinoma, despite a high recurrence rate and low survival rate. For patients with advanced cholangiocarcinoma, palliative care is the only option. However, the overall clinical benefit of palliative chemotherapy remains limited, with a median overall survival of 11.7 months [2], and even when combined with monoclonal antibodies against epidermal growth factor receptor (EGFR), the efficacy remains limited [3]. Next-generation sequencing (NGS) has identified previously unknown molecular characteristics and several new therapeutic targets of cholangiocarcinoma, such as fibroblast growth factor receptor 2 (*FGFR2*) gene fusion

and rearrangement, isocitrate dehydrogenase-1 (*IDH-1*) mutations [4], but only few fortunate patients carry these genetic changes, respectively 7.1% and 10.2% [5]. Although immunotherapy with programmed cell death protein 1 (PD-1) or programmed death-ligand 1 (PD-L1) antibodies has improved the therapeutic effect on many solid tumors [6], such as melanoma, lung cancer, and hepatocellular carcinoma, no satisfactory effect has been achieved for cholangiocarcinoma, with the median survival extended by only 1.3 months [7]. Therefore, treatments with higher efficacy are urgently needed.

Chimeric antigen receptor-T (CAR-T) cells have achieved great results in hematological tumors [8] and are being explored in a subset of solid tumors [9]. CAR-T cells have also been used in cholangiocarcinoma, with the main antigen targets being EGFR, human epidermal growth factor receptor 2 (HER2), mucin-1 (MUC-1), and glypican-3 (GPC3) [10]. EGFR overexpression is induced

by mutations in the receptor tyrosine kinase erythroblastic leukemia viral oncogene homolog (ERBB) family, which is implicated in tumor cell activation and uncontrolled cell division [11]. A clinical trial of CAR-T cell therapy targeted the EGFR antigen of cholangiocarcinoma and found that among 17 patients, 1 experienced complete remission while 10 had stable disease, suggesting CAR-T cells as a therapy for patients with cholangiocarcinoma [12]. The expression of another novel therapeutic target, B7 homolog 3 (B7H3), is increased in multiple solid tumors, including cholangiocarcinoma, but is limited in healthy tissues [13]. B7H3 is a type I transmembrane protein and a T cell costimulatory molecule. Previous studies showed that B7H3 mediates the inhibition of the tumor antigen-specific immune response and participates in tumor progression or escape [14–17].

Currently, CAR-T cell therapy faces various challenges in solid tumors. First, when CAR-T cells only target a single antigen, considerable parts of the tumor cells can escape from the CAR-T-cell-mediated killing owing to their genetic heterogeneity. Second, the tumor microenvironment (TME) contains a mass of tumor-associated fibroblasts and stromal cells that intercross each other and form a physical barrier [18, 19]. CAR-T cells do not have enough receptors to bind the chemokines generated from tumor cells or immune cells in the TME, thereby limiting their ability to infiltrate the TME [20]. Fortunately, CAR-T cell modifications, such as interleukin (IL)-7 and C-C motif chemokine ligand 21 (CCL21) overexpression, can improve immune cell infiltration [21]. CAR-T cells engineered to express IL-8 receptors, C-X-C motif chemokine receptor 1 (CXCR1), or C-X-C motif chemokine receptor 2 (CXCR2) showed markedly superior immune cell migration and persistence [22]. Finally, the TME remains highly immunosuppressive. This includes immune checkpoints and myeloid immunosuppression, causing premature CAR-T cell exhaustion and limiting efficacy [23, 24]. Our previous research demonstrated that the immune checkpoint pathway-modified CAR-T cells exert stronger antitumor activity in ovarian cancer [25].

In this study, we re-engineered PTG-T16R-scFv-CAR-T cells (CAR-T cells with decreased expression of PD-1, T-cell immunoglobulin and mucin domain-3 [Tim-3], T cell immunoglobulin and ITIM domain [Tigit], transforming growth factor β receptor [TGFβR], interleukin-10 receptor [IL-10R], and interleukin-10 receptor [IL-6R]) targeting EGFR and B7H3, based on the specific immunosuppressive microenvironment of cholangiocarcinoma. We then evaluated the antitumor immunity of these engineered CAR-T cells. We tested the antitumor activity and long-term efficacy of these cells versus conventional CAR-T cells using both in vitro and in vivo models of cholangiocarci-

noma. We expected that the PTG-T16R-scVF-CAR-T cells will be a valuable tool for solid tumor immunotherapy and contribute to solving technical challenges.

2 | MATERIALS AND METHODS

2.1 | Cell lines

Human embryonic kidney cell line HEK293T, human cholangiocarcinoma cell line TFK-1 and HuCCT1, and human acute T-lymphocytic leukemia cell line Jurkat were obtained from American Type Culture Collection (ATCC, Manassas, VA, USA). HEK293T and TFK-1 cell lines were cultured in Dulbecco's modified Eagle medium (DMEM; GIBCO, ThermoFisher Scientific, Beijing, China) supplemented with 10% fetal bovine serum (FBS; GIBCO) and 1% penicillin-streptomycin (GIBCO) at 37°C with 5% CO_2. HuCCT1 and Jurkat cell lines were cultured in RPMI-1640 medium (GIBCO) supplemented with 10% FBS and 1% penicillin-streptomycin at 37°C with 5% CO_2. Cell lines were confirmed for surface expression of target antigens and routinely tested for mycoplasma.

2.2 | Purification and culture of primary human CD8$^+$ T lymphocytes

Peripheral blood mononuclear cells (PBMCs) were derived from samples obtained from healthy volunteers by Ficoll-Hypaque gradient separation. This study was approved by the Clinical Ethics Review Board of the Third Affiliated Hospital of Sun Yat-sen University (permit number [2021]02-119 and [2022]02-077). Between March 2021 and December 2022, peripheral blood samples were collected from healthy volunteers with normal specific blood gravity and negative for human immunodeficiency virus (HIV), syphilis, hepatitis B virus, and hepatitis C virus. Primary human CD8$^+$ T cells were purified from PBMCs using enrichment set DM (BD-IMag^{TM}, Cat No. 557941, BD Biosciences) according to instructions. The main steps are described as follows: PBMCs were mixed with the Biotinylated Human CD8$^+$ T Lymphocyte Enrichment Cocktail, which simultaneously label red blood cells, platelets, and most white blood cells except CD8$^+$ T lymphocytes, at 5 μL per million cells at room temperature for 15 min. The labeled cells were washed twice, and the same volume of the BD IMag™ Streptavidin Particles Plus–DM was incubated with the cells at room temperature for 30 min. Then, the labeled cells were enriched by cell separation magnets, and unlabeled CD8$^+$ T cells in the remaining supernatant were collected. The sorted CD8$^+$ T lymphocytes were cultured in lymphocyte serum-free medium KBM581

(Corning, New York, NY, USA) supplemented with 1% penicillin-streptomycin at 37°C with 5% CO_2 and activated by 2 μg/mL anti-CD3 antibody (Ab) (Cat No. 317326, Biolegend, San Diego, CA, USA) and 1 μg/mL anti-CD28 Ab (Cat No. 302934, Biolegend). The transduced T cells were expanded in KBM581 medium supplemented with 1% penicillin-streptomycin, 2 mmol/L GlutaMAX (GIBCO), 0.1 mmol/L nonessential amino acids (GIBCO) at 37°C with 5% CO_2. Cells were fed with 10 ng/mL recombinant hIL-2 (Cat No. BT-002-050, R&D Systems, Minneapolis, MN, USA) every 3 days.

2.3 | Construction of CAR-encoding lentiviral vectors

The anti-EGFR single-chain fragment variable (scFV) was derived from the basic sequence of cetuximab (US20140304029, Samsung Electronics Co., Ltd., Suwon-si, Korea). The anti-B7H3 scFv was derived from mAb 376.96 [26, 27]. The scFv region was fused with the endodomains of CD28 (nucleotides 460-660; NM_006139.3), CD137 (nucleotides 640-765; NM_001561.5), and CD3ζ (nucleotides 160-492; NM_198053.2). As mock CAR-T cells, GP120-CAR targets the gp120 antigen of HIV-1 with sequences from a previous study [28]. Lentiviral vectors carrying an EGFR- or B7H3-specific CAR moiety and one or both of PTG/T16R shRNA derived from the miR-106b cluster were constructed. The PTG-shRNA cluster target PD-1, Tim-3, and Tigit genes, and the T16R-shRNA cluster target TGFβRII, IL-10RA, and IL-6R genes. Sequences of small interfering RNA (siRNA) are listed in Supplementary Table S1.

2.4 | Transduction of recombinant lentiviral particles

Plasmids encoding various CAR moieties, pMD.2G encoding VSV-G envelope, and a packaging vector plasmid psPAX2 were co-transfected into HEK293T cells prepared in a petri dish using the phosphate transfection system (Beyotime, Shanghai, China). The pseudotyped lentiviral supernatant was collected and filtered through a 0.45 μm membrane after 48 h. Pseudoviruses were concentrated via ultracentrifugation at 827,000 $\times$ g for 2 h at 4°C [25]. After activated for 48-72 h, CD8$^+$ T lymphocytes were transduced with pseudoviruses, supplemented with polybrene (Sigma-Aldrich, Saint Louis, MO, USA) at 8 μg/mL and centrifuged at 350 $\times$ g and 37°C for 90 min. After 12 h, CD8$^+$ T lymphocytes were fed in the fresh medium as described above.

2.5 | Quantitative reverse transcription PCR (qRT-PCR) and immunoblotting

Total RNA was extracted from modified CAR-T cells with TRIZOL reagent (Ambion, Carlsbad, CA, USA) and served as the template for preparing cDNA using a PrimeScript reverse transcription reagent kit (TaKaRa, Osaka, Japan). Primers for real-time qRT-PCR are listed in Supplementary Table S1. The results of the RNA relative expression were reported using the CFX96 Real-Time System (Bio-Rad, Singapore) and normalized with β-actin housekeeping gene used as an endogenous control.

HEK293T cells were transfected with CAR-encoding lentiviral plasmids. After 48 h, the cells were cleaved with NP40 buffer containing a cocktail of protease inhibitors (Beyotime, Shanghai, China). The lysate was collected, added to SDS loading buffer (GBCBIO, Guangzhou, Guangdong, China), and boiled for immunoblotting. The samples were added to 4%-12% SurePAGE (Genscript, Nanjing, Jiangsu, China) for electrophoresis. The protein was transferred from the gel to the nitrocellulose transfer membrane (HUAYUN, Guangzhou, Guangdong, China). They were then blocked with bovine serum albumin (BSA; MRC, Changzhou, Jiangsu, China) and incubated with primary antibodies (25°C, 1 h) and corresponding secondary antibodies (25°C, 30 min). The antibodies used were monoclonal mouse anti-flag (DYKDDDDK tag) mAb (1:5000, Cat No. 66008-4-Ig, Proteintech, Wuhan, Hubei, China), polyclonal rabbit anti-GAPDH mAb (1:5000, Cat No. 10494-1-AP, Proteintech), goat anti-rabbit IRDye 800CW (1:5000, Cat No. 926-32211, Li-cor, Lincoln, NE, USA), and goat anti-mouse IRDye 680RD (1:5000, Cat No. 926-68070, Li-cor). Images of immunoblotting were obtained using the two-color infrared laser imaging system Odyssey (Li-cor) and analyzed using Li-cor image studio software (Li-cor).

2.6 | Flow cytometric analysis

Fresh tumor tissues were collected from patients who underwent surgery for cholangiocarcinoma at the Third Affiliated Hospital of Sun Yat-sen University (Guangzhou, Guangdong, China). This study was approved by the Clinical Ethics Review Board of the Third Affiliated Hospital of Sun Yat-sen University (permit number [2021]02-119 and [2022]02-077). The following were the inclusion criteria: (1) all patients underwent surgical resection for cholangiocarcinoma; (2) all patients were pathologically diagnosed with cholangiocarcinoma between March 2021 and December 2021. The exclusion criteria included: (1) patients with two or more primary malignancies;

(2) patients with incomplete clinical information. The characteristics of enrolled patients with cholangiocarcinoma are shown in Supplementary Table S2. Isolation and collection of tissue mononuclear cells were performed as previously reported [29]. For analysis of the cell phenotypes, cells were stained in PBS containing 0.5% BSA (MRC, Changzhou, Jiangsu, China) and indicated antibody with a volume of 5 μL per million cells in 100 μL staining volume. Mouse anti-human AF647-EGFR (Cat No. 563577, BD Biosciences) and PE-CD276 (B7H3) (Cat No. 331605, Biolegend) were used to detect surface antigens of tumor cell lines and tumor tissues. For T-cell phenotypes in tumor tissues, the following antibodies were used: mouse anti-human APC-CD8a (Cat No. 17-0086-42, eBioscience, San Diego, CA, USA), PE/CY7-PD-1 (Cat No. 561272, BD Biosciences), Brilliant Violet 421-Tim-3 (Cat No. 565536, BD Biosciences), PE-Lag3 (Cat No. 12-2239-41, eBioscience), PerCP-eFluor 710-Tigit (Cat No. 46-9500-42, eBioscience), PE/CY7-BTLA (Cat No. 344516, Biolegend), PerCP-eFluor 710-CTLA4 (Cat No. 46-1529-42, eBioscience), Pacific Blue-CD244 (Cat No. 329524, Biolegend) and PE-CD160 (Cat No. 12-1609-42, eBioscience). Mouse anti-human Pacific Blue -CD8 (Cat No. 301033, Biolegend), FITC-CCR7 (Cat No. 11-1979-42, eBioscience), PerCP/CY5.5-CD45RO (Cat No. 304221, Biolegend) were used in in vivo experiment of xenogenic mouse models. The cell phenotypes were tested by Fluorescence Activated Cell Sorter (FACS, BD Biosciences), and data were analyzed with FlowJo software (Tree Star, Ashland, NC, USA).

2.7 | Cytotoxicity assay

To evaluate the ability of modified CAR-T cells to kill antigen-specific tumor cells, lactate dehydrogenase (LDH; Promega, Madison, WI, USA) release assay was used. Briefly, modified CAR-T cells were co-cultured with tumor cell lines at different ratios (from 10:1 to 0.625:1) for 24 h in a 96-well V-bottom plate. The LDH released was measured using the CytoTox96 Non-Radioactive Cytotoxicity Assay (Promega) according to the manufacturer's instructions. Absorbance values of wells were measured at 490 nm and subtracted as the background from the values of co-cultures. Cytotoxicity was calculated using the following formula: Cytotoxicity (%) = (Experimental value − Effector spontaneous value − Target spontaneous value)/ (Target maximum value − Target spontaneous value) × 100%. In the spontaneous group, effector and target cells were cultured alone. Target cells alone were lysed with a lysis reagent at 37°C for 30 min as a maximum control [25].

2.8 | Cholangiocarcinoma organoids culture and organoid killing assay

The main procedures were conducted as previously described [30]. Briefly, fresh human cholangiocarcinoma tumor tissue was cleaned, cut into small pieces, and digested into cell clumps that were suspended in Matrigel (basement membrane matrix, Corning) at 37°C for 20 min. After the matrix solidified, organoid cells were covered with fresh organoid medium. It was composed of Advanced DMEM/F12 (GIBCO) supplemented with 1% penicillin-streptomycin, 2 mmol/L GlutaMAX, 0.1 mmol/L nonessential amino acids, 10 mmol/L HEPES (GIBCO), 1:50 B27 supplement without vitamin A (GIBCO), 1:100 N2 supplement (GIBCO), 10 mmol/L nicotinamide (Sigma-Aldrich), 1.5 mmol/L N-Acetylcysteine (Sigma-Aldrich), 10 nmol/L recombinant human [Leu15]-Gastrin I (Sigma-Aldrich), 5 μmol/L A8301 (Sigma-Aldrich), 50 ng/mL human recombinant EGF (ThermoFisher Scientific, Waltham, MA, USA), 50 ng/mL human recombinant HGF (ThermoFisher Scientific), 50 ng/mL human recombinant FGF-10 (ThermoFisher Scientific), 10 μmol/L Y-27632(Sigma-Aldrich), and 30% Wnt3a-conditioned medium. Cholangiocarcinoma organoids were replaced with fresh medium every three days, dissociated by TrypLE Express (GIBCO) and passaged approximately once a week.

To evaluate the efficacy of autologous modified CAR-T cells against organoid cells, effector and target organoid cells were co-cultured in a 96-well plate at a 10:1 ratio. Firstly, organoid cells were dissociated into single cells and counted, and 1×10^4 organoid cells were inoculated in each well. Then CAR-T cells were labeled with 1 mmol/L of CellTrace Farred (Invitrogen, Carlsbad, CA, USA) and co-cultured with target cells. In the co-culture system, a green-fluorescent caspase 3/7 probe (Invitrogen) was added at 1:2000 dilution to indicate cell apoptosis. After 24 h of co-culture, micro-photographs images were taken by BioTek-lionheart FX (BioTek, Winooski, VT, USA). Finally, cells were washed in PBS and analyzed by flow cytometric analysis.

2.9 | Xenogenic mouse models

All mice experimental procedures were approved by the Institutional Animal Care and Use Committee of Sun Yat-sen University (permit number 2022000283). To establish a humanized mouse model, 6-week-old female NSG (NOD-Prkdc^{scid}IL2rg^{em1}/Smoc mice were purchased from Shanghai Model Organisms Co. Ltd (Shanghai, China) and raised normally in specific pathogen free (SPF) animal laboratory

at Sun Yat-sen University (permit number SYXK (YUE) 2010-0107). NSG mice were intravenously (i.v.) injected with 1×10^7 human fresh PBMCs and inoculated subcutaneously (s.c.) into the right flank with 5×10^6 TFK-1 cells in 100 μL PBS [31]. After 7 days, 1×10^6 modified homologous CAR-T cells were adoptively transferred into tumor-bearing mice intravenously (i.v.). All mice were intraperitoneally (i.p.) infused with recombinant hIL-2 (Cat No. BT-002-050, R&D Systems, Minneapolis, MN, USA) at 1 μg per mouse every 3 days. We observed the state of the mice, measured tumor size with calipers, and weighed the mice every 3 days. Once death, weakness or the tumor burden reached >1,500 mm^3 (Volume of tumor = length $\times$ width^2/2), mice were euthanized with carbon dioxide narcosis and cervical dislocation. At day 28, the tumor were dissected and digested with 2 mg/mL collagenase type IV (Sigma-Aldrich) at 37°C for 30 min. Cell suspensions were then passed through 70 μm filters and tumor-infiltrating lymphocytes (TILs) were separated via centrifugation on a discontinuous Percoll gradient (GE Healthcare, Cytiva, USA) and collected for subsequent experiments. A portion of mouse spleens was taken for physical dissection and lysis of red blood cells (RBCs) for subsequent use.

2.10 | Intracellular staining

To label CAR-T cells in mice, TILs and spleen cells from the PTG-T16R-EGFR-CAR-T and EGFR-CAR-T groups were co-incubated with 400 ng Recombinant Human EGFR (Cat No. CI61, NovoProtein, Suzhou, Jiangsu, China) in 50 μL at Room Temperature (RT) for 30 min. Similarly, TILs and spleen cells from GP120-CAR-T group were co-incubated with 400 ng Recombinant HIV gp120-8His (Cat No. CP93, NovoProtein) under the same conditions. Then anti-human APC-EGFR was indicated for CAR-T cells in the PTG-T16R-EGFR-CAR-T and EGFR-CAR-T groups, and PE-anti-His (Cat No. 362603, Biolegend) was indicated for CAR-T cells in the GP120-CAR-T groups. After extracellular staining, CAR-T cells were fixed and permeabilized using BD Cytofix/Cytoperm kit (BD Bioscience, San Jose, CA, USA) according to the manufacturer's instructions, and the anti-human Pacific Blue-IFN-γ (Cat No. 48-7319-42, eBioscience) was used for intracellular staining. Stained samples were tested using flow cytometric analysis and analyzed with FlowJo software.

2.11 | Immunohistochemistry (IHC)

Paraffin-embedded tissues of cholangiocarcinoma patients were collected from the pathology department of the Third Affiliated Hospital of Sun Yat-sen University. The following were the inclusion criteria: (1) all patients underwent surgical resection for cholangiocarcinoma; (2) all patients were pathologically diagnosed with cholangiocarcinoma between January 2016 and January 2017. The exclusion criteria included: (1) patients with two or more primary malignancies; (2) patients with incomplete clinical information. This study was approved by the Clinical Ethics Review Board of the Third Affiliated Hospital of Sun Yat-sen University (permit number [2021]02-119 and [2022]02-077). The characteristics of enrolled patients with cholangiocarcinoma are shown in Supplementary Table S3. The paraffin-embedded tissue was sectioned and stained according to standard procedures of Biopathology Institute Co., Ltd (Servicebio, Wuhan, Hubei, China). Briefly, paraffin-embedded tissue blocks were sectioned into 4-6 μm slices, followed by deparaffinized and rehydrated. Then tissue sections were incubated in a 10 mmol/L citrate buffer (pH = 6.0) at 95°C -100°C for 10 min for antigen retrieval. The tissue sections were then blocked with BSA and incubated with primary antibodies (4°C, overnight) and corresponding secondary antibodies (25°C, 30 min). The antibodies used were monoclonal mouse anti-human B7H3 mAb (1:5000, Cat No. 66481-1-Ig, Proteintech), monoclonal mouse anti-human EGFR mAb (1:200, Cat No.AF6043, Affinity Biosciences, Changzhou, Jiangsu, China) and anti-mouse IgG HRP-conjugated antibody (1:200, Cat No. GB23301, Servicebio). Images of IHC sections were obtained using the microscope (Pannoramic MIDI, 3DHISTECH, Budapest, Hungary). Positive controls were known immunostaining-positive slides, while negative controls were the staining slides with non-immune serum immunoglobulins instead of the primary antibody. For the assessment of antigen staining, the staining intensity was scored as follows [32]: negative (score 0), bordering (score 1), weak (score 2), moderate (score 3) and strong (score 4). The staining extent was graded into five parts according to the percentage of elevated staining cells in the field: negative (score 0), 0%–25% (score 1), 26%–50% (score 2), 51%–75% (score 3) and 76%-100% (score 4). The expression scores of EGFR and B7H3 were assessed by combined detection of staining intensity and extent.

After 28 days in vivo in xenogeneic mouse models, we assessed some organs from the euthanized mice, including the heart, liver, spleen, lung, kidney, stomach, small intestine large intestine, and pancreas. Samples were fixed with 4% formalin and embedded in paraffin; the sections were then stained with hematoxylin and eosin (H&E) staining (Biopathology Institute Co., Ltd, Servicebio). Images of H&E staining samples were obtained using a microscope (DM6000B, Leica, Wetzlar, Hessen, Germany) and (AxioScan.Z1, Carl Zeiss Microscopy GmbH, Oberkochen,

BV, Germany). The stained samples were analyzed using ZEN 2.3 software (Carl Zeiss Microscopy GmbH) and CaseViewer 2.4 software (3DHISTECH).

2.12 | Statistical Analysis

Experiments were conducted independently at least three times. Software GraphPad Prism 7.0 (GraphPad Software, San Diego, CA, USA) was used to process and analyze the data, which are presented as mean $\pm$ standard error of the mean (SEM). Two-tailed student's t-test was used to compare two independent groups, while one-way ANOVA was used in Tukey's multiple comparisons. Kaplan-Meier Curve was used to estimate the survival analysis of mice. Statistically significant differences were considered at $P < 0.05$.

3 | RESULTS

3.1 | EGFR-CAR-T cells and B7H3-CAR-T cells exhibited general antitumor activity

We collected surgical tumor tissues from patients with cholangiocarcinoma for the detection of EGFR and B7H3 antigen expression. The IHC showed that the expressions of both EGFR and B7H3 were abundant in cholangiocarcinoma tumor tissues (Figure 1A-B). These results prompted the selection of EGFR and B7H3 as the target molecules for cholangiocarcinoma-specific CAR-T development.

We then synthesized scFV sequences encoding anti-human EGFR and anti-human B7H3. The scFv regions were fused to a third-generation CAR moiety and inserted into lentiviral vectors (Figure 1C). The efficient expression of the EGFR-CAR and B7H3-CAR cassettes was verified by immunoblotting (Figure 1D). To generate EGFR-CAR-T cells and B7H3-CAR-T cells, we first generated the pseudotyped lentiviral particles from HEK293T cells, then infected activated human CD8$^+$ T lymphocytes. To further evaluate the EGFR-CAR and B7H3-CAR function, we co-cultured CAR-T cells with the cholangiocarcinoma cell lines TFK-1 and HuCCT1 respectively (Supplementary Figure S1A-B). The Jurkat cells that do not express EGFR or B7H3 antigens were used as negative controls. Both EGFR-CAR-T cells and B7H3-CAR-T cells showed dose-dependent and specific cytotoxicity to TFK-1 and HuCCT1 cells as measured by the LDH release assay. The cytotoxic effect was only 35%-37% at an effector-to-target (E:T) ratio of 10:1 (Figure 1E-F). Accordingly, the scFV-CAR-T cells should be further modified to improve their antitumor activity.

3.2 | Screening for highly abundant immune checkpoints in cholangiocarcinoma microenvironment

We modified CAR-T cells specifically for immunosuppressive conditions in the cholangiocarcinoma TME, mainly through immune checkpoints and immunosuppressive receptors on TILs. However, the immune microenvironments of malignant tumors are highly heterogeneous. To specifically screen the immune checkpoints of TILs in cholangiocarcinoma, we collected surgical tumor tissues and separated them for digestion. We detected the expression of PD-1, Tim-3, Lag3, Tigit, BTLA, CTLA4, CD244, and CD160 on TILs in the tumor, paratumor, and normal tissues from the same patient respectively by flow cytometric. In most patients, the expressions of immune checkpoints increased from the proximity to the center of the tumor (Figure 2A-I). Synchronous comparison of TILs in the same tumor tissue revealed that PD-1, Tigit, and Tim-3 were the three most expressed immune checkpoints we evaluated (Figure 2J) and were therefore selected to be downregulated specifically for cholangiocarcinoma CAR-T cells.

In addition, immune map characterization of cholangiocarcinoma has revealed that highly abundant immunosuppressive molecules TGFβ, IL-10, and IL-6 induced TIL dysfunction and mediated tumor escape by activating their corresponding receptors on TILs [33, 34]. Therefore, another strategy was to knock down the receptors of TGFβ, IL-10, and IL-6 on CAR-T cells. By blocking the immunosuppressive pathways mediated by them, these modifications could enhance the antitumor activity of CAR-T cells.

3.3 | The PTG-T16R-scFV-CAR-T cells exerted potent antitumor activity in vitro

The hsa-miR-106b cluster skeleton was used to place the specific shRNAs to knock down three genes simultaneously, as previously described [25]. We obtained PD-1, Tim-3, and Tigit shRNA sequences from previous reports [25, 35]. We screened shRNA sequences of TGFβR, IL-10R, and IL-6R using the siRNA construction library (Figure 3A). The PTG-shRNA cluster was designed to knock down the *PD-1*, *Tim-3*, and *Tigit* genes, while the T16R-shRNA cluster was designed to knock down the *TGFβRII*, *IL-10RA*, and *IL-6R* genes. The 3 constructed lentiviral vectors, named PTG-EGFR-CAR, T16R-EGFR-CAR, and PTG-T16R-EGFR-CAR, carry an EGFR-CAR moiety and a cluster of PTG-shRNA, T16R-shRNA, or both. The B7H3-CAR vector was constructed and named in the
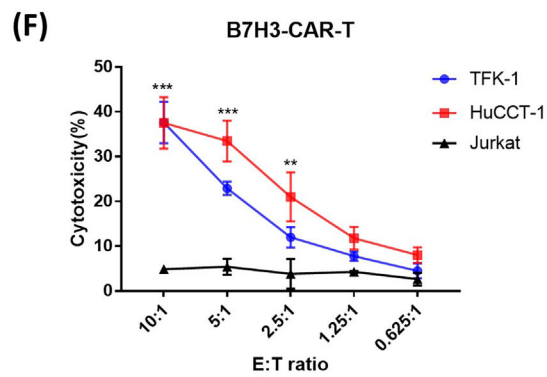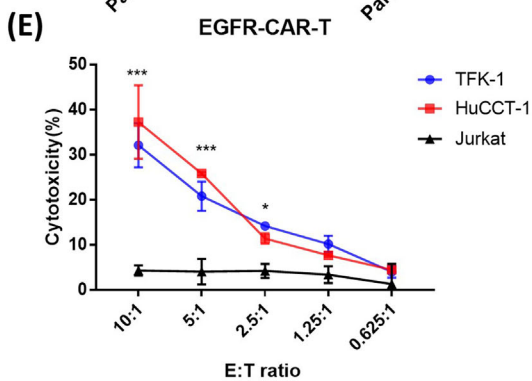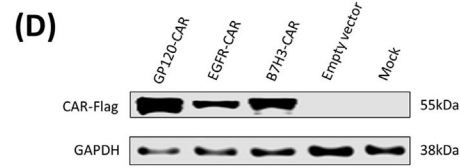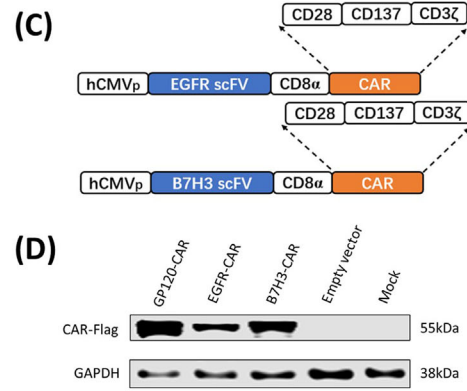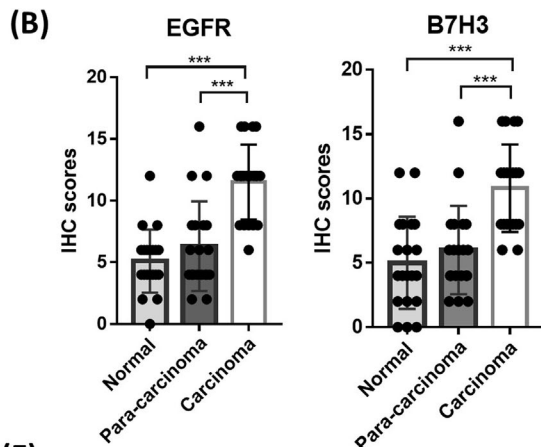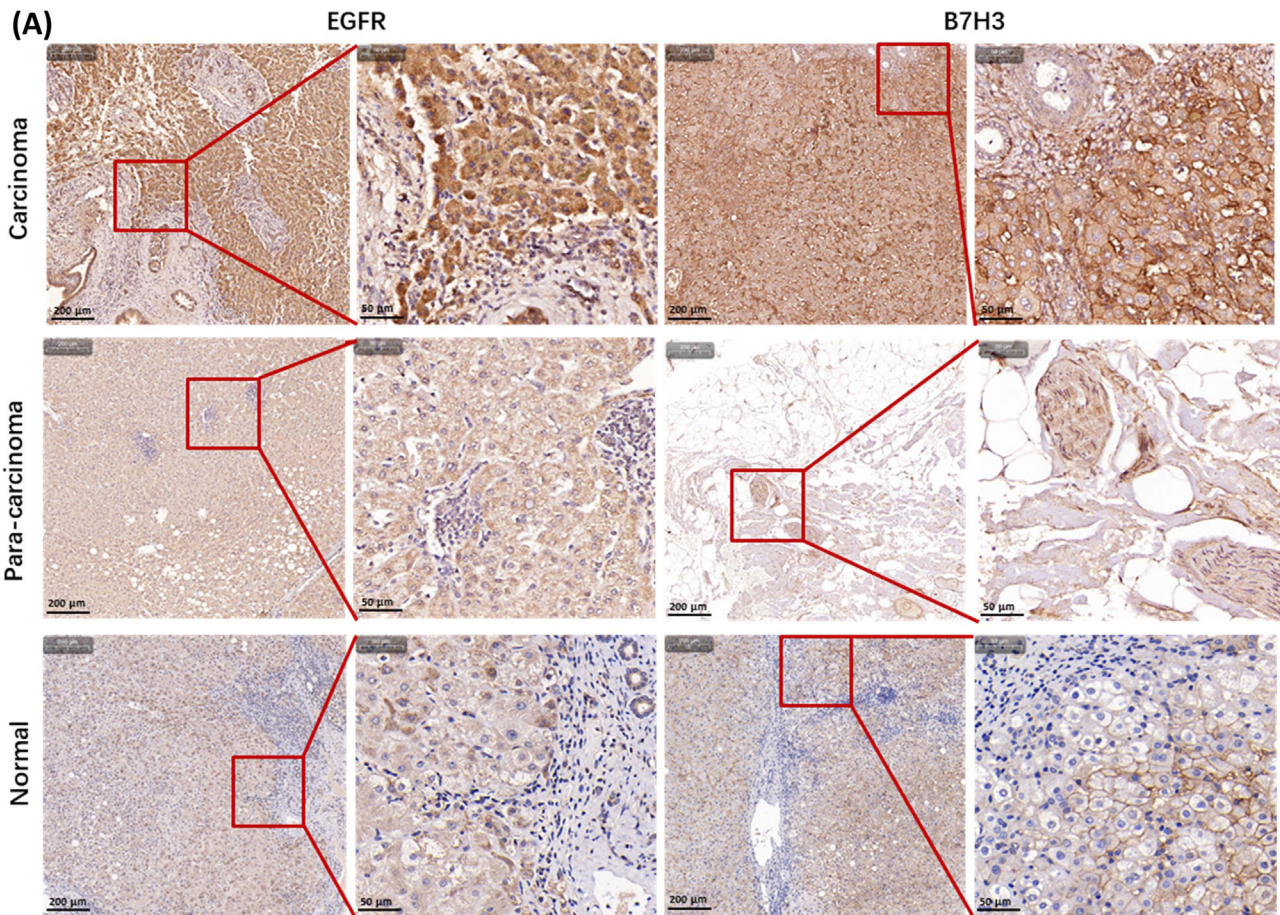
same manner (Figure 3B). The expressions of EGFR-CAR and B7H3-CAR after the addition of the shRNA cluster in lentiviral vectors were verified via immunoblotting (Figure 3C).

Gene knockdown efficiency of the PTG-T16R-scFV-CAR lentiviral vector was determined and transduced into activated CD8$^+$ T cells, followed by measuring the PD-1, Tim-3, Tigit, TGFβRII, IL-10R, and IL-6R expression levels through qRT-PCR. The multiple shRNA cluster-engineered CAR-T cells successfully downregulated 60%-75% of these 6 genes simultaneously (Supplementary Figure S2). In addition, we found that knockdown efficiency did not affect CAR-T cell growth (Supplementary Figure S3A) or infection efficiency (Supplementary Figure S3B).

We determined whether CAR-T cells exhibited improved antitumor activity after modifying the signaling pathways that mediate immunosuppression. Modified EGFR-CAR-T cells in each group were co-cultured separately with EGFR-antigen-positive TFK-1 and HuCCT1 cells. The GP120-CAR-T cells targeting HIV-1-infected cells were used as negative controls. The results of LDH assays indicated that the PTG-T16R-EGFR-CAR-T cells had the highest antitumor activity in vitro, followed by the PTG-EGFR-CAR-T cells, the T16R-EGFR-CAR-T cells, and lastly EGFR-CAR-T cells (Figure 3D). The modified B7H3-CAR-T cells yielded similar results (Figure 3E). These results demonstrate that the PTG-T16R-scFV-CAR-T cells exhibited potent antitumor activity in vitro.

3.4 | The PTG-T16R-B7H3-CAR-T cells exerted potent antitumor activity in a cholangiocarcinoma organoid-T cell co-culture system

Although cell lines are commonly used as in vitro models, their simplicity does not reflect actual TME. Therefore, we established cholangiocarcinoma organoids to further restore the original spatial relationships, functions, and characteristics of tumor tissues (Figures 4A-B).

We used cholangiocarcinoma organoids to reassess the antitumor capacity of CAR-T cells modified with multiple shRNA clusters in vitro. Autologous CAR-T cells were labeled with CellTrace Farred and cultured with the digested cholangiocarcinoma organoids. To detect the organoid apoptotic signals, we added the caspase 3/7 probe and monitored apoptosis activity by detecting FITC fluorescence using the real-time Biotech imaging system. After collating images of experimental groups at different time points, we observed that the GP120-CAR-T cells induced apoptosis to the weakest extent. The PTG-B7H3-CAR-T cells had stronger antitumor activity than the B7H3-CAR-T cells. The PTG-T16R-B7H3-CAR-T cells also exhibited the most potent tumor-killing ability, surrounding the organoids and causing a larger apoptotic area in the organoid center (Figure 4C). After 24 h, the flow cytometric analysis with the FITC-labeled caspase 3/7 probe indicated that the PTG-T16R-B7H3-CAR-T cells were the strongest mediators of tumor apoptosis (Figure 4D). Compared with the cell line co-culture, these organoid data generally yielded inferior results, possibly because tumor tissues obtained from cholangiocarcinoma patients could not fully express the B7H3 antigen (Supplementary Figure S1C). Nevertheless, this result indicates that cholangiocarcinoma organoids can be used to establish in vitro models that better reflect the complexity and persistence of clinical tumors.

3.5 | The PTG-T16R-scFV-CAR-T cells enhanced antitumor immunity in vivo

To verify the antitumor immunity of the PTG-T16R-scFV-CAR-T cells in vivo, we established a humanized mouse model. Humanized NSG mice were subcutaneously inoculated with TFK-1 cells and simultaneously transfused with human PBMCs to simulate the human immune system in a short time (Figure 5A).

Seven days after establishing the model, TFK-1 tumor-bearing mice were infused with either the PTG-T16R-EGFR-CAR-T cells, the EGFR-CAR-T cells, or the

FIGURE 1 EGFR-CAR T cells and B7H3-CAR T cells exhibited general antitumor activity in cholangiocarcinoma cell lines. (A-B) Detection of tumor tissue antigens collected from patients with cholangiocarcinoma by IHC staining. The left and right panels of A displayed representative EGFR and B7H3 expression in normal, para-carcinoma area, and tumor zone with enlarged view (5x, scale bar = 200 μm; 20x, scale bar = 50 μm). Statistical analysis of EGFR and B7H3 antigens scores in normal, para-carcinoma and carcinoma tissues (B, $n = 20$). (C) Schematic representation of the lentiviral vectors carrying an EGFR-specific 3rd generation CAR moiety (EGFR-CAR) and a B7H3-specific 3rd generation CAR moiety (B7H3-CAR). (D) Immunoblotting analysis of EGFR-CAR and B7H3-CAR expression were performed with anti-flag tag. The positive control was GP120-CAR. (E-F) Detection cytotoxic activities of the EGFR-CAR-T cells and the B7H3-CAR-T cells with TFK-1 cells and HuCCT1 cells by LDH assay. The negative control was Jurkat cells without EGFR and B7H3 expression ($n = 3$, healthy donors). Experiments were performed independently at least 3 times. One-way ANOVA was used in Tukey's multiple comparison test. Experimental data are expressed as mean $\pm$ SEM. *, $P < 0.05$; **, $P < 0.01$; ***, $P < 0.001$.

Abbreviations: CAR, chimeric antigen receptor T; EGFR, epidermal growth factor receptor; B7H3, B7 homolog 3; GP120, gp120 antigen; IHC, immunohistochemistry; LDH, lactate dehydrogenase; SEM, standard error of the mean.
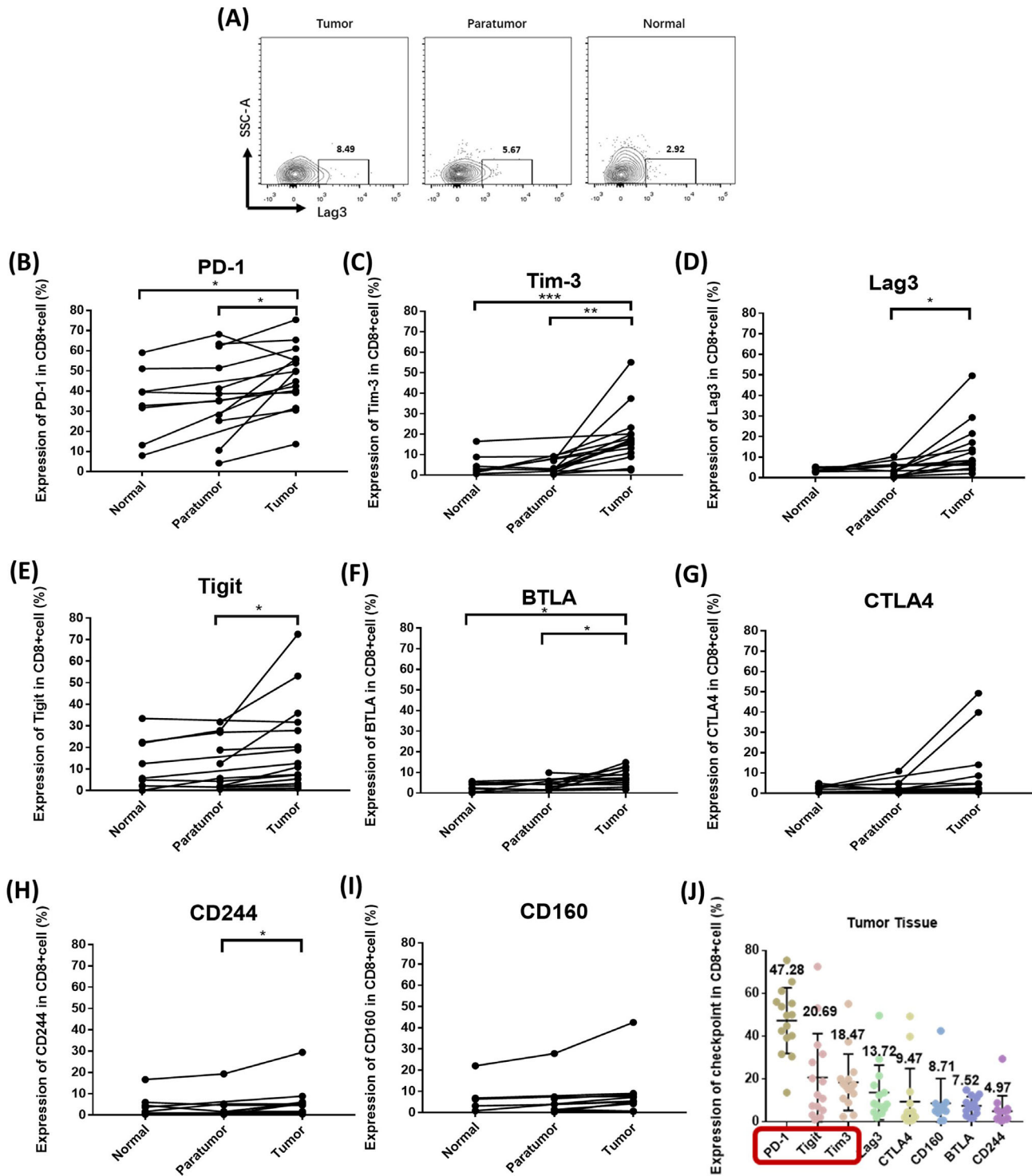
FIGURE 2 Screening of immune checkpoints on CD8$^+$ TILs in cholangiocarcinoma microenvironment. (A) Representative flow plots of immune checkpoints on CD8$^+$ TILs. The proportion of Lag3$^+$ cells in CD8$^+$ TILs of tumor tissue, paratumor tissue, and normal tissue from one patient. (B-I) Quantitative analysis of immune checkpoints on CD8$^+$ TILs. PD-1 (B), Tim-3 (C), Lag3 (D), Tigit (E), BTLA (F), CTLA4 (G), CD244 (H), and CD160 (I) were detected by flow cytometric analysis respectively. The connecting lines indicated that the tissue came from one patient ($n = 15$). (J) Statistical analysis of immune checkpoints on CD8$^+$ TILs in cholangiocarcinoma tissue. Experiments were performed independently at least 3 times. Paired two-tailed student's t-test was used to compare two non-independent groups. Experimental data are expressed as mean ± SEM. *, $P < 0.05$; **, $P < 0.01$; ***, $P < 0.001$.

Abbreviations: TIL, tumor-infiltrating lymphocyte; PD-1, programmed death-1; Tim-3, T-cell immunoglobulin and mucin domain-3; Tigit, T cell immunoglobulin and ITIM domain; Lag3, lymphocyte activation gene 3; BTLA, B and T lymphocyte attenuator; CTLA4, cytotoxic T lymphocyte-associated protein-4; SEM, standard error of the mean.
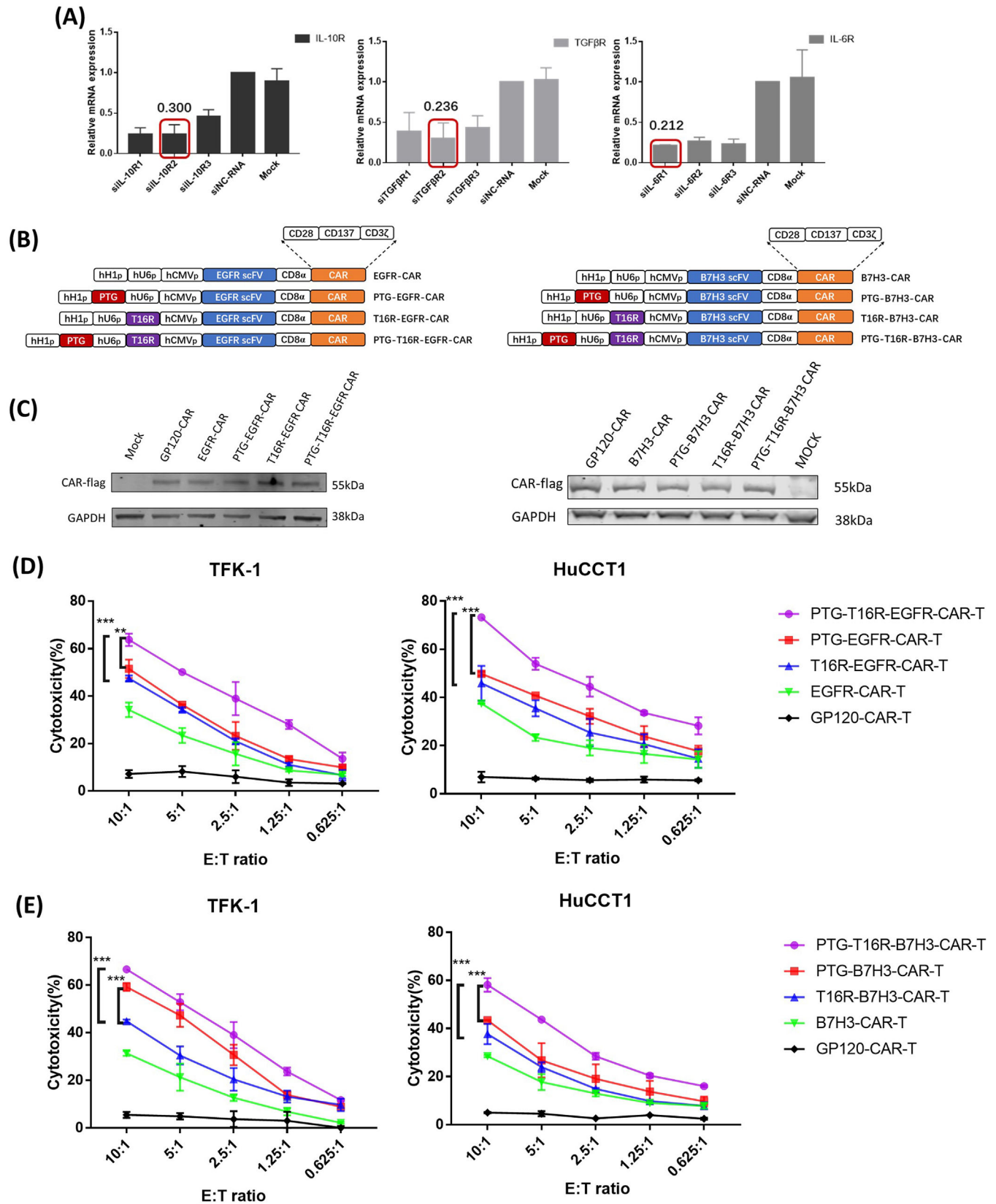
FIGURE 3 The PTG-T16R-scFV-CAR T cells exerted potent antitumor activity in vitro, (A) siRNA mediated immunosuppressive factor receptors knockdown efficiency screening in HEK293T cells by qPT-PCR: including targeted *TGFβRII*, *IL-10RA* and *IL-6R* genes. The red boxes represented the siRNA with the highest knockdown efficiency. (B) Left schematic representation of the lentiviral vectors carrying an EGFR-CAR moiety and a cluster of PTG-shRNA or T16R-shRNA, or both. Right schematic representation showed the same modification of

negative-control GP120-CAR-T cells. Tumor size was measured in 3-day intervals; mice were euthanized after 28 days. The resulting data demonstrated the antitumor ability of EGFR-CAR-T cells, but antitumor properties could be further enhanced through engineering the PTG-T16R-EGFR-CAR-T cells that synchronously knocked down immune checkpoints and immunosuppressive receptors (Figure 5B). Subsequently, the subcutaneous tumors were removed from mice and digested with collagenase. We used indirect FACS to detect tumor-infiltrating CAR-T cells, and found that the PTG-T16R-EGFR-CAR-T group had 28.5% tumor-infiltrating CAR-T cells, while the EGFR-CAR-T group had 15.0%, suggesting that CAR-T cells with multiple shRNA clusters showed greater infiltrative and/or local proliferative abilities in cholangiocarcinoma tumors (Figure 5C). In addition, tumor-infiltrating PTG-T16R-EGFR-CAR-T cells secreted a higher level of IFN-γ (Figure 5D), a cytokine that mediates apoptosis and enhances antitumor immunity. Moreover, we found an increased proportion of central memory CAR-T cells in the spleen treated with the PTG-T16R-EGFR-CAR-T cells, rather than in the EGFR-CAR-T group (Figure 5E). This result suggests that the PTG-T16R-EGFR-CAR-T cells are of higher homing ability and memory persistence, which allows them to survive longer in vivo and achieve long-term antitumor effects.

To further compare the antitumor immunity of the modified B7H3-CAR-T cells, we transfected humanized cholangiocarcinoma mice with five groups of engineered B7H3-CAR-T cells, then conducted long-term observations of tumor size, body weight, and survival status. Our findings support the superior antitumor activity of the PTG-T16R-B7H3-CAR-T cells, with the PTG-B7H3-CAR-T cells possessing slightly lower antitumor activity, although still greater than the T16R-B7H3-CAR-T cells and the B7H3-CAR-T cells (Figure 5F). The TFK-1 tumor-bearing mice treated with the PTG-T16R-B7H3-CAR-T cells had significantly better survival, followed by the PTG-B7H3-CAT-T group (Figure 5G). Mouse weight did not change significantly and the function of major organs ware normal during the evaluation period (Figure 6, Supplementary Figures S4-S5), implying the safety of modified CAR-T cells. Collectively, these results demonstrated that the PTG-T16R-scFV-CAR-T cells exhibited potent antitumor activity in vivo.

4 | DISCUSSION

The novel design and functional mechanism make CAR-T cell therapy an integral part of the treatment of malignant tumors. CAR-T cells targeting CD19 have been approved as a treatment for leukemia and lymphoma due to their high efficacy by the United States Food and Drug Administration, European Medicines Agency and China National Medical Products Administration. There also have been many exploratory studies on solid tumors with gratifying results. For example, Claudin18.2 (CLDN18.2)-redirected CAR-T cells acquired 48.6% overall response rate (ORR) against gastric cancer [36]. In the next few years, CAR-T cell therapy is bound to make further strides in solid tumors. For cholangiocarcinoma, the safety and efficacy of EGFR-CAR-T cells have been established in a phase I clinical study [12]. In addition, B7H3-specific CAR-T cells are effective in multiple preclinical models, including neuroblastoma, osteosarcoma, medulloblastoma, Ewing sarcoma, atypical teratoid/rhabdoid tumors, and NK/T cell lymphoma [27, 37-39]. In this study, B7H3 overexpression in cholangiocarcinoma tumor cells was observed, as high as 95.7% in one clinical sample. Given the heterogeneity of tumor cells, a CAR-T cocktail containing immunotherapies for different targets is a feasible treatment for cholangiocarcinoma that could relieve off-target effects, although further study for potential toxicity is required [40].

---

the lentiviral vectors carrying B7H3-CAR. The PTG-shRNA cluster can target the knockdown of *PD-1*, *Tim-3*, and *Tigit* genes and the T16R-shRNA cluster can target the knockdown of *TGFβRII*, *IL-10RA* and *IL-6R* genes. These cluster skeletons were derived from the miR-106b cluster in human genome. (C) The expressions of EGFR-CAR and B7H3-CAR after shRNA clusters modification were analyzed by immunoblotting with anti-flag tag. The positive control was GP120-CAR. (D) The cytotoxic activities of the PTG-T16R-EGFR-CAR-T cells, the PTG-EGFR-CAR-T cells, the T16R-EGFR-CAR-T cells, the EGFR-CAR-T cells and the GP120-CAR-T cells co-cultured with TFK-1 or Hucct1 cells were compared by LDH assay. The negative control was the GP120-CAR-T cells group ($n = 3$, healthy donors). (E) The cytotoxic activities of the PTG-T16R-B7H3-CAR-T cells, the PTG-B7H3-CAR-T cells, the T16R-B7H3-CAR-T cells, the B7H3-CAR-T cells and the GP120-CAR-T cells co-cultured with TFK-1 or Hucct1 cells were compared by LDH assay. The negative control was the GP120-CAR-T cells group ($n = 3$, healthy donors). Experiments were performed independently at least 3 times. One-way ANOVA was used in Tukey's multiple comparison test. Experimental data are expressed as mean ± SEM. *, $P < 0.05$; **, $P < 0.01$; ***, $P < 0.001$.

Abbreviations: siRNA, small interfering RNA; TGFβR, transforming growth factor β receptor; IL-10R, interleukin 10 receptor; IL-6R, interleukin 6 receptor; PD-1, programmed death-1; Tim-3, T-cell immunoglobulin and mucin domain-3; Tigit, T cell immunoglobulin and ITIM domain; CAR, chimeric antigen receptor T; EGFR, epidermal growth factor receptor; B7H3, B7 homolog 3; GP120, gp120 antigen; LDH, lactate dehydrogenase; SEM, standard error of the mean.
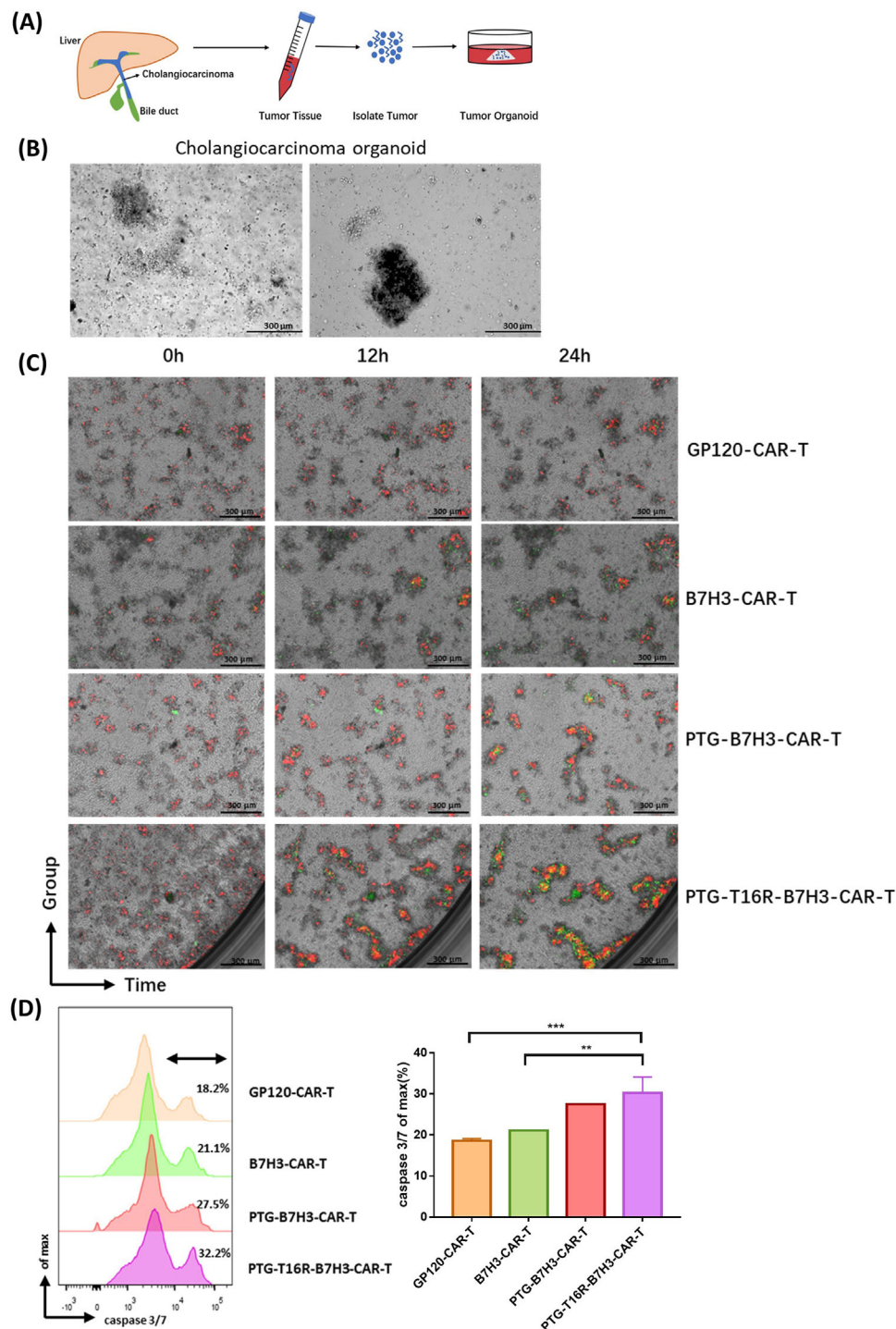
FIGURE 4 The PTG-T16R-B7H3-CAR-T cells exerted potent antitumor activity in cholangiocarcinoma organoid-T cell co-culture system. (A) Schematic diagram of cholangiocarcinoma organoid model. (B) Brightfield microscopy images of cholangiocarcinoma organoid. Scale bar: 300 μm. (C) The PTG-T16R-B7H3-CAR-T cells, PTG-B7H3-CAR-T cells, B7H3-CAR-T cells, and GP120-CAR-T cells co-cultured with autologous tumor cholangiocarcinoma organoid for 24 h, separately. CAR-T cells (red) were labeled with Cell-trace Farred and apoptotic cells (green) were labeled with caspase-3/7 probe. Real-time Biotech imaging system was used to take one picture per hour for 24 h. The GP120-CAR-T cells served as negative control. Scale bars: 300 μm. (D) Representative flow plots of cholangiocarcinoma organoid apoptosis by caspase 3/7 probe (FITC). The quantification of organoid apoptosis in organoid-T cell co-culture system by flow cytometric analysis. Experiments were performed independently at least 3 times. One-way ANOVA was used in Tukey's multiple comparison test. Experimental data are expressed as mean $\pm$ SEM. **, $P < 0.01$; ***, $P < 0.001$.

Abbreviations: CAR-T, chimeric antigen receptor T; B7H3, B7 homolog 3; GP120, gp120 antigen; SEM, standard error of the mean.
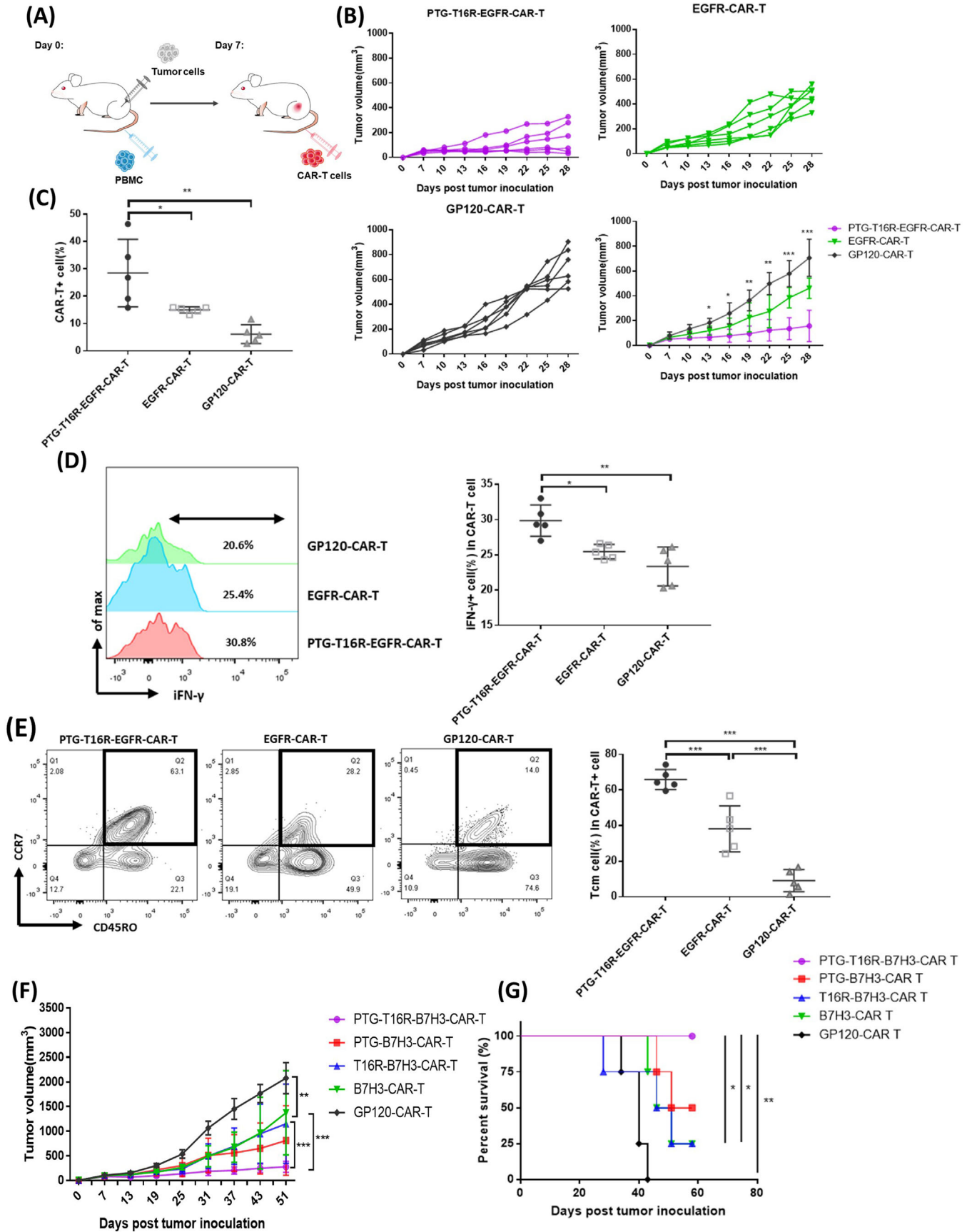
The exhaustion of CAR-T cells has been a prominent limitation in the treatment of solid tumors, and many studies have been conducted to overcome this difficulty. Either the combination of CAR-T cells with checkpoint antibodies or the down-regulation of intrinsic PD-1 in CAR-T cells enhances their antitumor properties [41, 42]. In this study, we first screened for the expression of immune checkpoints in tumor-infiltrating T cells from cholangiocarcinoma patients, aiming to improve CAR-T efficacy in this specific tumor tissue. Our results indicated that PD-1, Tigit, and Tim-3 were the top three among various immune checkpoints. This outcome is in line with a previous study showing that the PD-1 antibody has a curative effect in cholangiocarcinoma [43], especially among patients with a defective DNA mismatch repair system [44]. Additionally, Tigit inhibits the activation of tumor-infiltrating T cells via binding to CD155 of dendritic cells and CD155-expressing tumor cells, blocking CD155-mediated activation of the co-stimulator CD226 [45, 46]. Nine human anti-Tigit antibodies exhibited potential in 43 phase-1/2/3 clinical trials as a treatment for advanced solid tumors, either as a monotherapy or in combination with anti-PD-1/PD-L1 antibodies or chemotherapies [47, 48]. Moreover, the humanized IgG4k antibody MBG453 of Tim-3 was designated as an orphan drug for myelodysplastic syndromes (MDS) treatment by the European Commission in August 2021, exhibiting a durable clinical response when administered to patients with extremely high-risk MDS (vHR/HR-MDS) and acute myeloid leukemia in combination with demethylation (HMAs) (2021, ASH). Clinical trials of Tim-3 antibody in patients with solid tumors are also in progress (NCT02817633, NCT04785820), showing considerable therapeutic potential.

In addition to the immune checkpoints, another dilemma with CAR-T treatment of solid tumors is the soluble immunosuppressive cytokines in the TME [49]. Based on this, we engineered CAR-T cells that simultaneously knocked down the immunosuppressive molecular receptors TGFβR, IL-10R, and IL-6R, and found that it increased antitumor activity. This effect is maximized when it is knocked down in conjunction with immune checkpoints (Figure 7). Other studies have also shown that CAR-T cell function is improved in TGF-β-enriched TMEs after knocking out endogenous TGFBR2, expressing TGF-β-receptor kinase inhibitor, or expressing dominant-negative TGFBRII [50–52]. Engineered CAR-T cells secreting bifunctional trap proteins targeting PD-1 and TGF-β also enhance antitumor immunity and efficacy [53]. Interrupting IL-10 signal pathway also increased anti-tumor immunity of CAR-T cells [54]. Other immunosuppressive cytokines, including IL-6, are present in the complex immunosuppressive TME of cholangiocarcinoma [55, 56]. In addition, monocytes secrete large amounts of inflammatory cytokines, including IL-6, after CAR-T cell therapy, triggering the life-threatening cytokine release syndrome (CRS) [57]. Tocilizumab is an IL-6 receptor blocker approved by the Food and Drug Administration to inhibit CRS, in line with our efforts to knock down IL-6 receptor expression in CAR-T cells in this study.

In this study, we overcame this immunosuppression with innovative PTG-T16R-scVF-CAR-T cells that simultaneously inhibit the expression of TGF-β, IL-10, and IL-6 receptors, as well as PD-1, Tigit, and Tim-3 with multiple shRNA clusters. Moreover, the proliferation and anti-tumor activity of CAR-T cells were almost not affected after shRNA clusters knockdown, but not knockout. This strategy led to a significant in vitro and in vivo antitumor effect, and a robust homing ability that can maintain the in vivo antitumor effects of CAR-T cells over the long term. Verification of the safety and effectiveness of the PTG-T16R-scVF-CAR-T cells in clinical trials is warranted to improve the treatment of cholangiocarcinoma.

This study has some limitations. The mechanism of memory PTG-T16R-scVF-CAR-T cell homing remains to

---

FIGURE 5 The PTG-T16R-scFV-CAR-T cells enhanced antitumor immunity in vivo. (A) Schematic diagram of humanized NSG mice cholangiocarcinoma model. (B-E) After subcutaneously inoculating humanized NSG mice with TFK-1 cells for 7 days, the mice were transfused with the PTG-T16R-EGFR-CAR-T cells, EGFR-CAR-T cells, and GP120-CAR-T cells via the tail vein. 28 days later, the mice were euthanized. Tumor size was measured using calipers every 3 days. The tumor volume of mice in the three groups was statistically analyzed (B; $n = 6$). The percentage of infiltrating CAR-T cells in tumor (C; $n = 5$). Statistical analysis of the intracellular cytokine staining for IFN-γ on infiltrating CAR-T cells in tumor (D; $n = 5$). Representative flow plots of central memory CAR-T cells (CD45RO$^+$CCR7$^+$) expression in the spleen of mice. The proportion of central memory CAR-T cells from three groups was statistically analyzed (E; $n = 5$). (F) Long-term evaluation of mice tumor volume after adoptive modification of CAR-T cells targeting B7H3 antigen ($n = 4$). (G) Kaplan-Meier survival analysis of mice. Death, weakness or tumor volume over 1500mm^3 were set as the end events. Experiments were performed independently at least 3 times. One-way ANOVA was used in Tukey's multiple comparison test. Experimental data are expressed as mean ± SEM. *, $P < 0.05$; **, $P < 0.01$; ***, $P < 0.001$.

Abbreviations: CAR, chimeric antigen receptor T; EGFR, epidermal growth factor receptor; B7H3, B7 homolog 3; GP120, gp120 antigen; IFN-γ, interferon-γ; SEM, standard error of the mean.
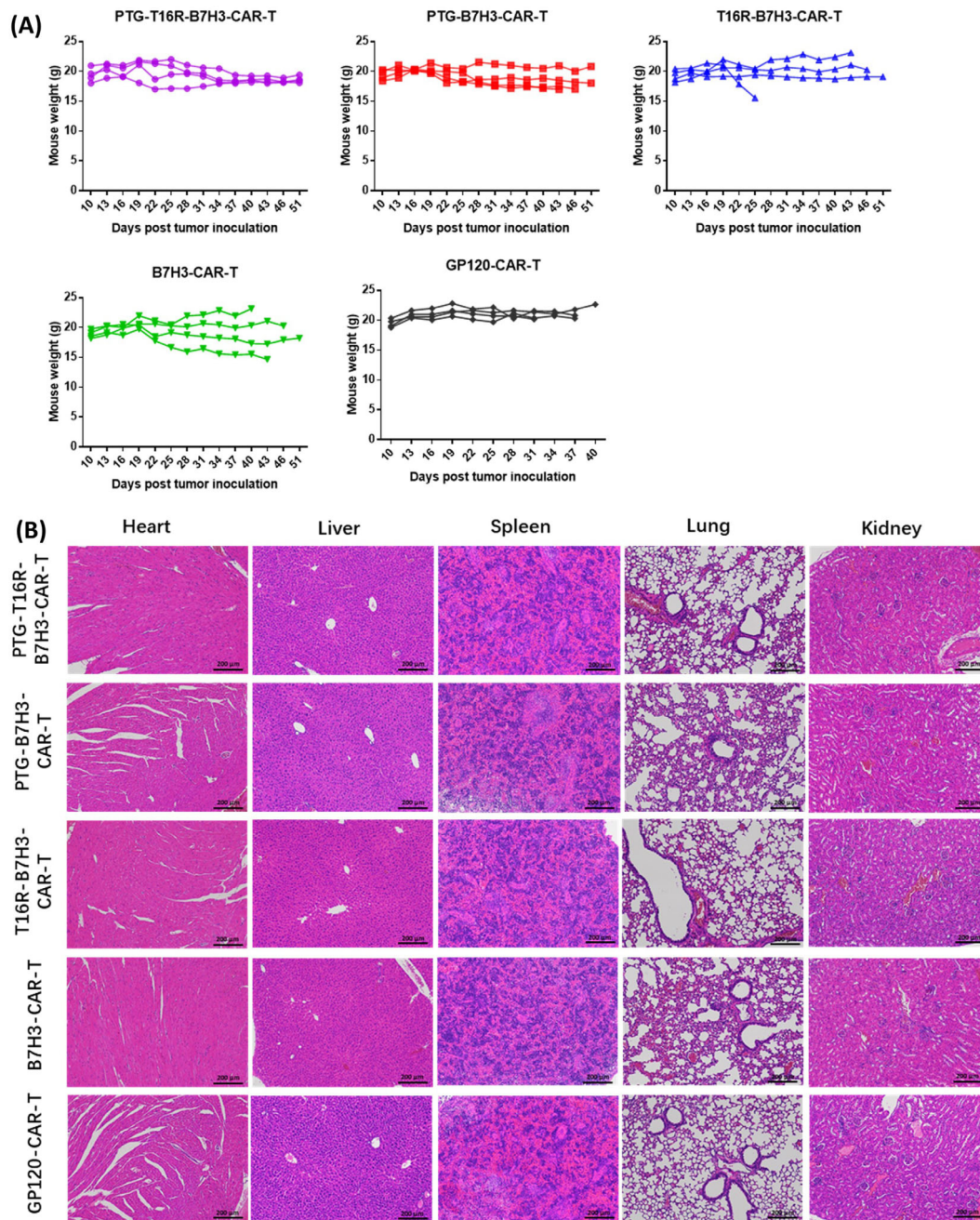
FIGURE 6 Safety evaluation of adoptive modified CAR-T cells in vivo, (A) After the PTG-T16R-B7H3-CAR-T cells, PTG-B7H3-CAR-T cells, T16R-B7H3-CAR-T cells, B7H3-CAR-T cells, and GP120-CAR-T cells were transfused to the mice, the mice were weighed every three days ($n = 4$). Each dot represents an individual data point. (B) H&E staining of major organ tissues in various groups' mice: the PTG-T16R-B7H3-CAR-T cell group, PTG-B7H3-CAR-T cell group, T16R-B7H3-CAR-T cell group, B7H3-CAR-T cell group, and GP120-CAR-T cell group. The tissues (heart, lung, liver, kidney, and spleen) were derived from humanized mice after 21 days of CAR-T cell transfusion. Abbreviations: CAR-T, chimeric antigen receptor T; EGFR, epidermal growth factor receptor; B7H3, B7 homolog 3; GP120, gp120 antigen; H&E, hematoxylin and eosin.

be elucidated. Although the PTG-T16R-scVF-CAR-T cells have been shown in our in vivo mouse model, their safety and efficacy warrant further confirmation in preclinical trials.

5 | CONCLUSIONS

In this study, we enhanced the CAR-T cell antitumor function through a novel engineering strategy that
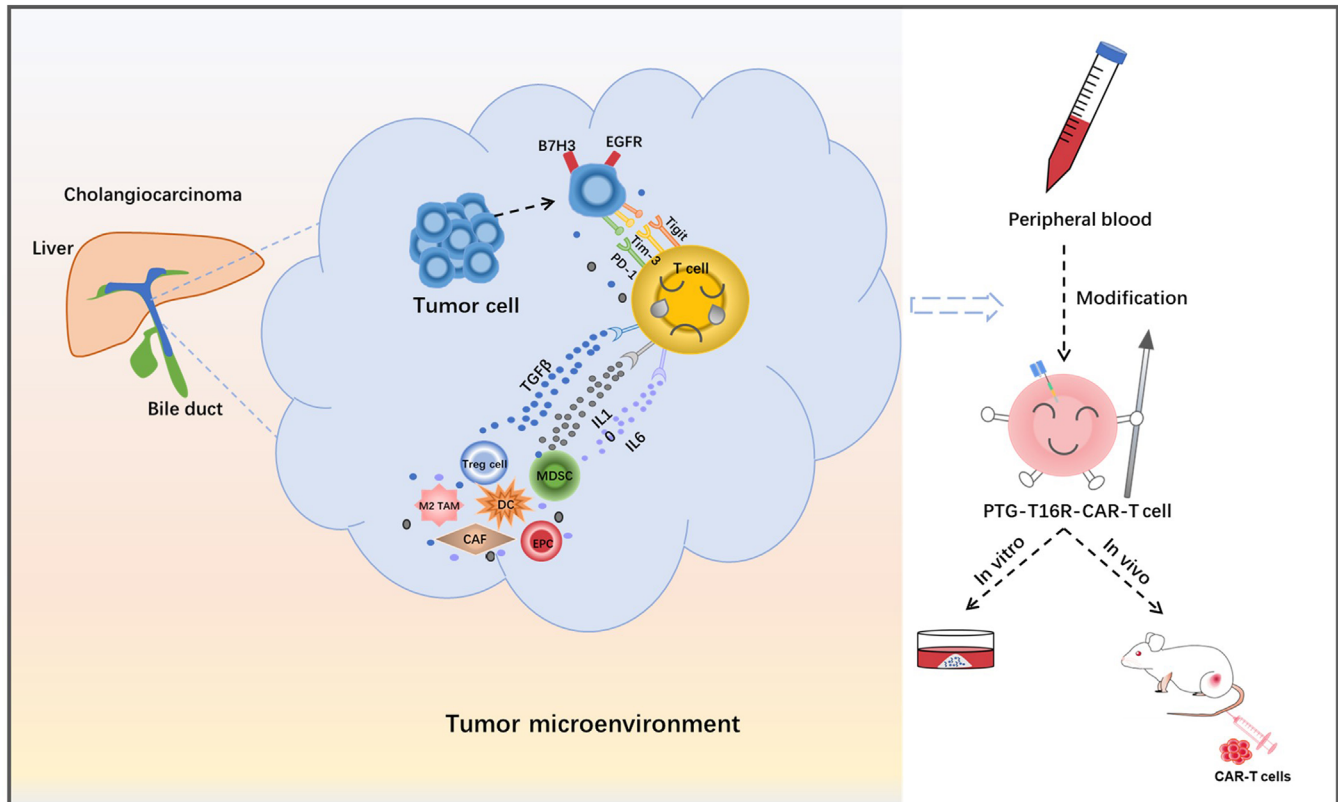
FIGURE 7 Schematic depiction of the PTG-T16R-CAR-T cells modification based on the cholangiocarcinoma TME. Abbreviations: CAR-T, Chimeric Antigen Receptor T; EGFR, Epidermal Growth Factor Receptor; PD1, Programmed Cell Death 1; Tim-3, T cell Immunoglobulin and Mucin Domain-containing Protein 3; Tigit, T Cell Immunoreceptor with Ig and ITIM Domains; TGFβR, Transforming Growth Factor Beta Receptor; IL, Interleukin; TME, Tumor Microenvironment.

combined the inhibitory effects of multiple checkpoints and immunosuppressive cytokine receptors. These CAR-T cells can improve the clinical outcome of patients with cholangiocarcinoma and possibly provide a general strategy for treating solid tumors.

DECLARATIONS

None.

AUTHOR CONTRIBUTIONS

Conceptualization, Lijuan Lu, Xiangyuan Wu, and Hui Zhang; methodology, Yidan Qiao, Jie Chen, Xuemei Wang, Baijin Xia, Keming Lin, and Xu Zhang; sample collection, Shumei Yan, Jizhou Tan, and Yongjian Chen; investigation, Fan Zou, Bingfeng Liu, Xin He, and Yiwen Zhang; writing–original draft, Yidan Qiao and Lijuan Lu; writing–review & editing, Xiangyuan Wu and Hui Zhang; supervision, Lijuan Lu. All authors revised and approved the manuscript.

ETHICS APPROVAL AND CONSENT TO PARTICIPATE

Mice experiments were approved by the Institutional Animal Care and Use Committee of Sun Yat-sen University (permit number 2022000283) and were carried out in concert with the guidelines and regulations of the Laboratory Monitoring Committee of Guangdong Province of China. Human peripheral blood of anonymous healthy blood donors was obtained from the Guangzhou Blood Center. All fresh tumor tissues and paraffin-embedded tissues were collected from patients underwent surgery of cholangiocarcinoma at the Third Affiliated Hospital of Sun Yat-sen University, Guangzhou, China. This study was approved by the Clinical Ethics Review Board of the Third Affiliated Hospital of Sun Yat-sen University (permit number [2022]02-077), the requirement to obtain informed consent was waived.

CONSENT FOR PUBLICATION

Not applicable.

DATA AVAILABILITY STATEMENT

All datasets generated or analyzed during this study have included in this manuscript. The data are available from the corresponding author on reasonable request.

ORCID

Yidan Qiao https://orcid.org/0000-0003-3219-6426
Xin He https://orcid.org/0000-0002-2131-2092

REFERENCES

1. Rizvi S, Khan SA, Hallemeier CL, Kelley RK, Gores GJ. Cholangiocarcinoma - evolving concepts and therapeutic strategies. Nat Rev Clin Oncol. 2018;15(2):95–111.
2. Valle J, Wasan H, Palmer DH, Cunningham D, Anthoney A, Maraveyas A, et al. Cisplatin plus gemcitabine versus gemcitabine for biliary tract cancer. N Engl J Med. 2010;362(14):1273–81.
3. Rizzo A, Frega G, Ricci AD, Palloni A, Abbati F, S DEL, et al. Anti-EGFR Monoclonal Antibodies in Advanced Biliary Tract Cancer: A Systematic Review and Meta-analysis. In Vivo. 2020;34(2):479–88.
4. Ricci AD, Rizzo A, Brandi G. The DNA damage repair (DDR) pathway in biliary tract cancer (BTC): a new Pandora's box? ESMO Open. 2020;5(5):e001042.
5. Abou-Alfa GK, Sahai V, Hollebecque A, Vaccaro G, Melisi D, Al-Rajabi R, et al. Pemigatinib for previously treated, locally advanced or metastatic cholangiocarcinoma: a multicentre, open-label, phase 2 study. Lancet Oncol. 2020;21(5): 671–84.
6. Wang Y, Wang M, Wu HX, Xu RH. Advancing to the era of cancer immunotherapy. Cancer Commun (Lond). 2021;41(9):803–29.
7. Rizzo A, Ricci AD, Brandi G. Durvalumab: an investigational anti-PD-L1 antibody for the treatment of biliary tract cancer. Expert Opin Investig Drugs. 2021;30(4):343–50.
8. Maude SL, Frey N, Shaw PA, Aplenc R, Barrett DM, Bunin NJ, et al. Chimeric antigen receptor T cells for sustained remissions in leukemia. N Engl J Med. 2014;371(16):1507–17.
9. Lou H, Cao X. Antibody variable region engineering for improving cancer immunotherapy. Cancer Commun (Lond). 2022;42(9):804–27.
10. Medicine USNLo. https://clinicaltrials.gov/
11. Schaft N. The Landscape of CAR-T Cell Clinical Trials against Solid Tumors-A Comprehensive Overview. Cancers (Basel). 2020;12(9):2567.
12. Guo Y, Feng K, Liu Y, Wu Z, Dai H, Yang Q, et al. Phase I Study of Chimeric Antigen Receptor-Modified T Cells in Patients with EGFR-Positive Advanced Biliary Tract Cancers. Clin Cancer Res. 2018;24(6):1277–86.
13. Li G, Wang H, Wu H, Chen J. B7-H3-targeted CAR-T cell therapy for solid tumors. Int Rev Immunol. 2022;41(6):625–37.
14. Kontos F, Michelakos T, Kurokawa T, Sadagopan A, Schwab JH, Ferrone CR, et al. B7-H3: An Attractive Target for Antibody-based Immunotherapy. Clin Cancer Res. 2021;27(5):1227–35.
15. Brustmann H, Igaz M, Eder C, Brunner A. Epithelial and tumor-associated endothelial expression of B7-H3 in cervical carcinoma: relation with CD8+ intraepithelial lymphocytes, FIGO stage, and phosphohistone H3 (PHH3) reactivity. Int J Gynecol Pathol. 2015;34(2):187–95.
16. Benzon B, Zhao SG, Haffner MC, Takhar M, Erho N, Yousefi K, et al. Correlation of B7-H3 with androgen receptor, immune pathways and poor outcome in prostate cancer: an expression-based analysis. Prostate Cancer Prostatic Dis. 2017;20(1):28–35.
17. Picarda E, Ohaegbulam KC, Zang X. Molecular Pathways: Targeting B7-H3 (CD276) for Human Cancer Immunotherapy. Clin Cancer Res. 2016;22(14):3425–31.
18. Martinez M, Moon EK. CAR T Cells for Solid Tumors: New Strategies for Finding, Infiltrating, and Surviving in the Tumor Microenvironment. Front Immunol. 2019;10:128.
19. Labanieh L, Majzner RG, Mackall CL. Programming CAR-T cells to kill cancer. Nat Biomed Eng. 2018;2(6):377–91.
20. Long KB, Young RM, Boesteanu AC, Davis MM, Melenhorst JJ, Lacey SF, e al. CAR T Cell Therapy of Non-hematopoietic Malignancies: Detours on the Road to Clinical Success. Front Immunol. 2018;9:2740.
21. Luo H, Su J, Sun R, Sun Y, Wang Y, Dong Y, et al. Coexpression of IL7 and CCL21 Increases Efficacy of CAR-T Cells in Solid Tumors without Requiring Preconditioned Lymphodepletion. Clin Cancer Res. 2020;26(20):5494–505.
22. Jin L, Tao H, Karachi A, Long Y, Hou AY, Na M, et al. CXCR1- or CXCR2-modified CAR T cells co-opt IL-8 for maximal antitumor efficacy in solid tumors. Nat Commun. 2019;10(1):4016.
23. Ngwa VM, Edwards DN, Philip M, Chen J. Microenvironmental Metabolism Regulates Antitumor Immunity. Cancer Res. 2019;79(16):4003–8.
24. Nakamura K, Smyth MJ. Myeloid immunosuppression and immune checkpoints in the tumor microenvironment. Cell Mol Immunol. 2020;17(1):1–12.
25. Zou F, Lu L, Liu J, Xia B, Zhang W, Hu Q, et al. Engineered triple inhibitory receptor resistance improves anti-tumor CAR-T cell performance via CD56. Nat Commun. 2019;10(1):4109.
26. Fauci JM, Sabbatino F, Wang Y, Londono-Joshi AI, Straughn JM Jr, Landen CN, et al. Monoclonal antibody-based immunotherapy of ovarian cancer: targeting ovarian cancer cells with

the B7-H3-specific mAb 376.96. Gynecol Oncol. 2014;132(1): 203–10.

27. Du H, Hirabayashi K, Ahn S, Kren NP, Montgomery SA, Wang X, et al. Antitumor Responses in the Absence of Toxicity in Solid Tumors by Targeting B7-H3 via Chimeric Antigen Receptor T Cells. Cancer Cell. 2019;35(2):221–37 e8.

28. Liu B, Zou F, Lu L, Chen C, He D, Zhang X, et al. Chimeric Antigen Receptor T Cells Guided by the Single-Chain Fv of a Broadly Neutralizing Antibody Specifically and Effectively Eradicate Virus Reactivated from Latency in CD4+ T Lymphocytes Isolated from HIV-1-Infected Individuals Receiving Suppressive Combined Antiretroviral Therapy. J Virol. 2016;90(21):9712–24.

29. Chen J, Qiao YD, Li X, Xu JL, Ye QJ, Jiang N, et al. Intratumoral CD45(+)CD71(+) erythroid cells induce immune tolerance and predict tumor recurrence in hepatocellular carcinoma. Cancer Lett. 2021;499:85–98.

30. Zou F, Tan J, Liu T, Liu B, Tang Y, Zhang H, et al. The CD39(+) HBV surface protein-targeted CAR-T and personalized tumor-reactive CD8(+) T cells exhibit potent anti-HCC activity. Mol Ther. 2021;29(5):1794–807.

31. Sanmamed MF, Rodriguez I, Schalper KA, Onate C, Azpilikueta A, Rodriguez-Ruiz ME, et al. Nivolumab and Urelumab Enhance Antitumor Activity of Human T Lymphocytes Engrafted in Rag2-/-IL2Rgammanull Immunodeficient Mice. Cancer Res. 2015;75(17):3466–78.

32. Wan XB, Fan XJ, Chen MY, Xiang J, Huang PY, Guo L, et al. Elevated Beclin 1 expression is correlated with HIF-1alpha in predicting poor prognosis of nasopharyngeal carcinoma. Autophagy. 2010;6(3):395–404.

33. Raggi C, Invernizzi P, Andersen JB. Impact of microenvironment and stem-like plasticity in cholangiocarcinoma: molecular networks and biological concepts. J Hepatol. 2015;62(1):198–207.

34. Andersen JB, Spee B, Blechacz BR, Avital I, Komuta M, Barbour A, et al. Genomic and genetic characterization of cholangiocarcinoma identifies therapeutic targets for tyrosine kinase inhibitors. Gastroenterology. 2012;142(4):1021–31 e15.

35. Lozano E, Dominguez-Villar M, Kuchroo V, Hafler DA. The TIGIT/CD226 axis regulates human T cell function. J Immunol. 2012;188(8):3869–75.

36. Qi C, Gong J, Li J, Liu D, Qin Y, Ge S, et al. Claudin18.2-specific CAR T cells in gastrointestinal cancers: phase 1 trial interim results. Nat Med. 2022;28(6):1189–98.

37. Majzner RG, Theruvath JL, Nellan A, Heitzeneder S, Cui Y, Mount CW, et al. CAR T Cells Targeting B7-H3, a Pan-Cancer Antigen, Demonstrate Potent Preclinical Activity Against Pediatric Solid Tumors and Brain Tumors. Clin Cancer Res. 2019;25(8):2560–74.

38. Theruvath J, Sotillo E, Mount CW, Graef CM, Delaidelli A, Heitzeneder S, et al. Locoregionally administered B7-H3-targeted CAR T cells for treatment of atypical teratoid/rhabdoid tumors. Nat Med. 2020;26(5):712–9.

39. Zheng M, Yu L, Hu J, Zhang Z, Wang H, Lu D, et al. Efficacy of B7-H3-Redirected BiTE and CAR-T Immunotherapies Against Extranodal Nasal Natural Killer/T Cell Lymphoma. Transl Oncol. 2020;13(5):100770.

40. Feng KC, Guo YL, Liu Y, Dai HR, Wang Y, Lv HY, et al. Cocktail treatment with EGFR-specific and CD133-specific chimeric antigen receptor-modified T cells in a patient with advanced cholangiocarcinoma. J Hematol Oncol. 2017;10(1):4.

41. John LB, Devaud C, Duong CP, Yong CS, Beavis PA, Haynes NM, et al. Anti-PD-1 antibody therapy potently enhances the eradication of established tumors by gene-modified T cells. Clin Cancer Res. 2013;19(20):5636–46.

42. Hu W, Zi Z, Jin Y, Li G, Shao K, Cai Q, et al. CRISPR/Cas9-mediated PD-1 disruption enhances human mesothelin-targeted CAR T cell effector functions. Cancer Immunol Immunother. 2019;68(3):365–77.

43. Ott PA, Bang YJ, Piha-Paul SA, Razak ARA, Bennouna J, Soria JC, et al. T-Cell-Inflamed Gene-Expression Profile, Programmed Death Ligand 1 Expression, and Tumor Mutational Burden Predict Efficacy in Patients Treated With Pembrolizumab Across 20 Cancers: KEYNOTE-028. J Clin Oncol. 2019;37(4):318–27.

44. Le DT, Uram JN, Wang H, Bartlett BR, Kemberling H, Eyring AD, et al. PD-1 Blockade in Tumors with Mismatch-Repair Deficiency. N Engl J Med. 2015;372(26):2509–20.

45. Yu X, Harden K, Gonzalez LC, Francesco M, Chiang E, Irving B, et al. The surface protein TIGIT suppresses T cell activation by promoting the generation of mature immunoregulatory dendritic cells. Nat Immunol. 2009;10(1):48–57.

46. Johnston RJ, Comps-Agrar L, Hackney J, Yu X, Huseni M, Yang Y, et al. The immunoreceptor TIGIT regulates antitumor and antiviral CD8(+) T cell effector function. Cancer Cell. 2014;26(6):923–37.

47. Chauvin JM, Zarour HM. TIGIT in cancer immunotherapy. J Immunother Cancer. 2020;8(2):e000957.

48. Ge Z, Peppelenbosch MP, Sprengers D, Kwekkeboom J. TIGIT, the Next Step Towards Successful Combination Immune Checkpoint Therapy in Cancer. Front Immunol. 2021;12:699895.

49. Turley SJ, Cremasco V, Astarita JL. Immunological hallmarks of stromal cells in the tumour microenvironment. Nat Rev Immunol. 2015;15(11):669–82.

50. Tang N, Cheng C, Zhang X, Qiao M, Li N, Mu W, et al. TGF-beta inhibition via CRISPR promotes the long-term efficacy of CAR T cells against solid tumors. JCI Insight. 2020;5(4):e133977.

51. Stuber T, Monjezi R, Wallstabe L, Kuhnemundt J, Nietzer SL, Dandekar G, et al. Inhibition of TGF-beta-receptor signaling augments the antitumor function of ROR1-specific CAR T-cells against triple-negative breast cancer. J Immunother Cancer. 2020;8(1):e000676.

52. Kloss CC, Lee J, Zhang A, Chen F, Melenhorst JJ, Lacey SF, et al. Dominant-Negative TGF-beta Receptor Enhances PSMA-Targeted Human CAR T Cell Proliferation And Augments Prostate Cancer Eradication. Mol Ther. 2018;26(7):1855–66.

53. Chen X, Yang S, Li S, Qu Y, Wang HY, Liu J, et al. Secretion of bispecific protein of anti-PD-1 fused with TGF-beta trap enhances antitumor efficacy of CAR-T cell therapy. Mol Ther Oncolytics. 2021;21:144–57.

54. Sullivan KM, Jiang X, Guha P, Lausted C, Carter JA, Hsu C, et al. Blockade of interleukin 10 potentiates antitumour immune function in human colorectal cancer liver metastases. Gut. 2023;72(2):325–337.

55. Isomoto H, Mott JL, Kobayashi S, Werneburg NW, Bronk SF, Haan S, et al. Sustained IL-6/STAT-3 signaling in cholangiocarcinoma cells due to SOCS-3 epigenetic silencing. Gastroenterology. 2007;132(1):384–96.

56. Fabris L, Sato K, Alpini G, Strazzabosco M. The Tumor Microenvironment in Cholangiocarcinoma Progression. Hepatology. 2021;73 (Suppl 1):75–85.

57. Norelli M, Camisa B, Barbiera G, Falcone L, Purevdorj A, Genua M, et al. Monocyte-derived IL-1 and IL-6 are differentially required for cytokine-release syndrome and neurotoxicity due to CAR T cells. Nat Med. 2018;24(6):739–48.

SUPPORTING INFORMATION

Additional supporting information can be found online in the Supporting Information section at the end of this article.